THERMAL DEPENDENCE OF SPIN-ORBIT TORQUE-INDUCED MAGNETIZATION REVERSAL IN PERMALLOY THIN FILM

Jun Fujioka,[1] Syuta Honda,[1]* Hiroyoshi Itoh,[1] and Yuichiro Ando[2]

(Received September 6, 2022; accepted November 25, 2022)

Abstract

The magnetization of a nanosized thin film reverses owing to the spin-orbit torque (SOT) induced via a spin injection from a heavy metal (HM). The magnetization reversal can be used as a magnetic-memory binary digit at temperatures above room temperature. We investigated magnetization reversal by means of SOT under the thermal effect using micromagnetic simulation. The thermal effect was introduced as random magnetic fields. The averaged magnetization reversal time decreased with increasing temperature. However, several samples exhibited exceptional oscillatory behavior of the magnetization during the reversal and the reversal times increased.

1 Introduction

The magnetization of ferromagnetic (FM) thin film can be used as a magnetic-memory binary digit, such as magnetoresistive random-access memory (MRAM), that is, the two magnetized directions can correspond to the two possible binary-digit values, "0" and "1." The magnetization reversal process occurs owing to the influence of spin-transfer torque (STT) induced via spin injected into the film.[1,2] When an electric current flows through a heavy metal (HM), which is lead on the film, the carrier spin polarizes due to the spin Hall effect via a spin-orbit interaction (Fig. 1(a)).[3,4] The polarized spin can then be injected into the film. The injected spin diffuses and acts on the magnetic moments of the film as a torque, resulting

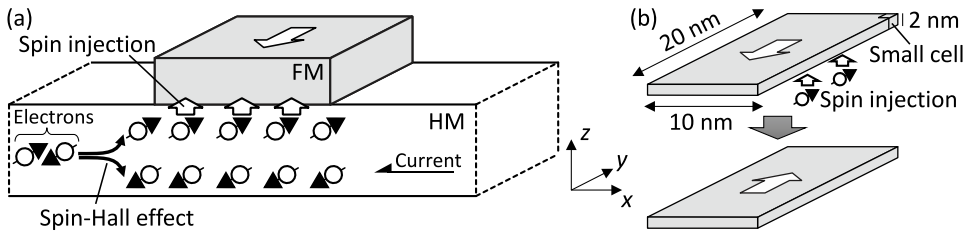

Fig. 1. Schematic of (a) the spin injection into the ferromagnetic metal (FM) from the heavy metal (HM) for the spin-orbit torque (SOT) and (b) magnetization reversal simulation.

1 Department of Pure and Applied Physics, Kansai University, Suita, Osaka 564-8680, Japan
2 Department of Electronic Science and Engineering, Kyoto University, Katsura, Kyoto 615-8510, Japan
* Correspondence to: Syuta Honda, Department of Pure and Applied Physics, Kansai University, Suita, Osaka 564-8680, Japan. E-mail: shonda@kansai-u.ac.jp

in magnetization reversal.[5-7)]

The spin-orbit torque (SOT) can be expected to reverse the magnetization under low power conditions. However, a strong magnetization reversal time dependence has been observed experimentally. It is known that the magnetization fluctuates under finite temperatures. This thermal fluctuation may affect the magnetization reversal. Consequently, in this study, we focused on the magnetization reversal of film owing to the SOT with thermal fluctuation. The variation in the magnetization reversal time was investigated using micromagnetic simulations, random magnetic fields being introduced in the simulation as thermal fluctuations.

2 Model and Methods

We applied a micromagnetic model base on the Landau-Lifshitz-Gilbert (LLG) equation to simulate the magnetization reversal of FM thin film owing to the SOT effect. The dimension of the thin film was set to 20 nm × 40 nm × 2.0 nm (Fig. 1(b)). The film was magnetized along the y-axis under the influence of magnetic shape anisotropy. The +y-polarized spin was injected from the bottom surface of the film. The injected spin affects the magnetization of the film as the SOT. The film was subdivided into 2.0 nm^3 cubic cells, the magnetization of which could be calculated using a version of the transposed LLG equation, expressed as follows (including the SOT term, which is the third term on the right-hand side):[8,9)]

$$\frac{d\boldsymbol{m}}{d\tau} = -|\gamma|\,\boldsymbol{m}\times\boldsymbol{B}_{\mathrm{eff}} - \alpha|\gamma|\,\boldsymbol{m}\times(\boldsymbol{m}\times\boldsymbol{B}_{\mathrm{eff}}) + (-\boldsymbol{m}\times(\boldsymbol{m}\times(-\nabla\cdot\boldsymbol{j}_{\mathrm{sot}}))), \quad (1)$$

where $\boldsymbol{m}$ denotes a unit vector representing the magnetization direction within each cell, τ denotes the simulation time, γ denotes the gyromagnetic ratio $\gamma = -1.76\times10^{11}$ rad s^{-1} T^{-1}, α denotes the Gilbert damping constant, and $\boldsymbol{B}_{\mathrm{eff}}$ denotes the effective magnetic field comprising long-range magnetic dipole-dipole interactions, short-range exchange interactions among the neighboring computational cells, and random magnetic fields for thermal fluctuations (thermal fields).

We applied the fourth-order Runge-Kutta method with a step-size ($\delta\tau$) of 0.01 ps for time integration in the simulation. The parameter values based on the properties of the permalloy were chosen as follows: α was set to 0.0073,[10)] the saturation magnetization M_s was 860 kA m^{-1}, the exchange stiffness constant A between adjacent magnetic moments was 13.0 pJ m^{-1}, [11,12)] and M_s and A were used to calculate the components of each magnetic field.

Thermal fields based on the Langevin equation ($\boldsymbol{B}_t$) were applied,[13,14)] with a spherically symmetrical random direction. The location- and time-averaged thermal field was $\langle\boldsymbol{B}_t\rangle = \boldsymbol{0}$, with each component of the thermal field having a normal distribution. The averaged magnitude of the thermal fields was $\langle|\boldsymbol{B}_t|\rangle = (2\alpha kT/(VM_s|\gamma|\delta\tau))^{1/2}$, where k denotes the Boltzmann constant, T denotes the temperature, and V denotes the cell volume. A temperature (T) of $0 \le T \le 400$ K was chosen.

The divergence of the SOT spin current ($\nabla\cdot\boldsymbol{j}_{\mathrm{sot}}$) can be defined as $-\nabla\cdot\boldsymbol{j}_{\mathrm{sot}} \equiv (0, -\partial u/\partial z, 0)$,[15,16)] where $\boldsymbol{j}_{\mathrm{sot}}$ is a tensor quantity with a spin-polarized direction and a spin current direction, and u is a spin velocity that has the dimension of m/s and describes the intensity of the spin current. Because the spin diffusion length of the FM, which is approximately 2 nm, is similar to the FM thickness and the film has only one cell that can be used for the direction of spin

injection, $-\partial u/\partial z$ can be approximated by $u_0/2.0$ nm,[16,17] where u_0 denotes the magnitude of the injection velocity of the spin current. u_0 was set to 30 m/s.[15]

3 Results and Discussion

First, we set the direction of all magnetic moments to the −y-direction. The magnetic moments relaxed by 0.5 ns without the SOT under the thermal field. Figure 2 shows one example of these states at each temperature. The magnetic moments mostly pointed in the −y-direction at $T=0$ K, that is, under conditions of a zero thermal field, as shown in Fig. 2(a). The magnetic moments at the corners of the film pointed slightly to the outside of the film due to the long-range dipole-dipole interactions. When a thermal field was applied, the magnetic moments canted slightly in various directions from the −y-direction (Fig. 2(b)-(f)), with the canting angle increasing with increasing T. Fortunately, the magnetization maintained the −y-direction even at 400 K. The values of the y-component of the averaged film magnetic moments $\langle m_y \rangle$ were −1.0 at $T=0$ K, −0.99 at 50 K, −0.98 at 100 K, −0.96 at 200 K, −0.92 at 300 K, and −0.91 at 400 K.

Magnetization reversal simulations were then conducted at a SOT of $u_0=30$ m/s at $T=0$ K. Figure 3 shows one example of the magnetization reversal process at $T=0$ K. The SOT begins

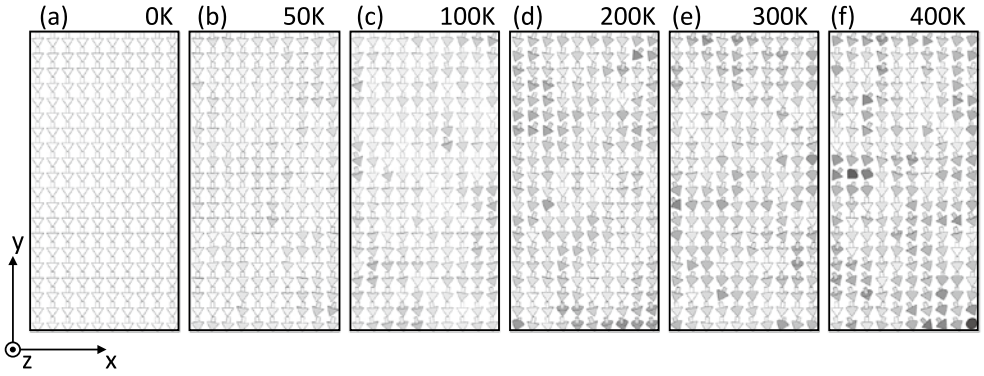

Fig. 2. Magnetic moments of the initial magnetic state of the permalloy film at (a) 0, (b) 50, (c) 100, (d) 200, (e) 300, and (f) 400 K; each small arrow indicates the direction of the magnetic moment. The shading of each arrow indicates the magnitude of the component in the y-direction. When the arrow is white, the magnetic moment points in the ±y-direction.

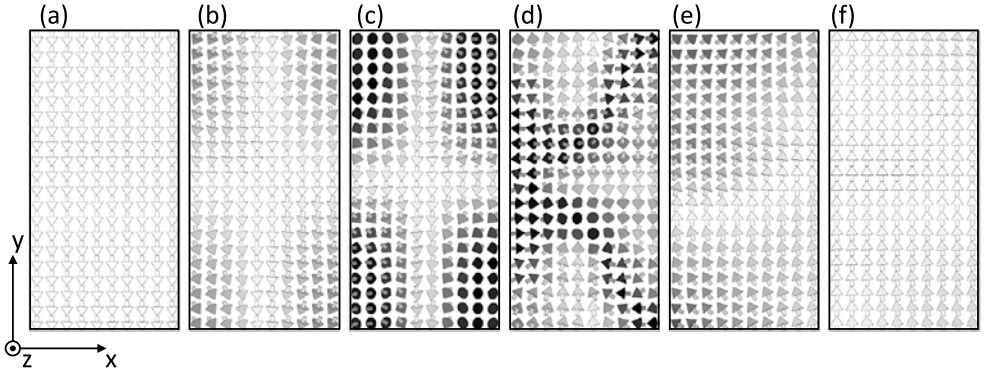

Fig. 3. Snapshots of the magnetization reversal process of the film at 0 K at τ = (a) 0, (b) 0.3, (c) 0.4, (d) 0.5, (e) 0.6, and (f) 0.7 ns; each small arrow indicates the direction of the magnetic moment.

to act on the 0.5 ns-relaxed magnetization ($\tau = 0$ ns). When $\tau = 0$ ns, the magnetic moments lay mostly in the −y-direction (Fig. 3(a)); at this point, the SOT hardly affected the magnetic moments. Fortunately, the magnetic moments canted slightly from the −y-direction at the corners of the film, as they absorbed the SOT. Next, the magnetic moments rotated symmetrically from the corner of the film under the influence of the SOT (Fig. 3(b)-3(e)). Most magnetic moments pointed in the +y-direction at $\tau = 0.7$ ns (Fig. 3(f)). Consequently, the magnetization reversed at $\tau = 0.61$ ns. Here, we define the time at which the $\langle m_y \rangle$ becomes 0.97 as the magnetization reversal time (τ_r).

Magnetization reversal with $T > 0$ K was conducted at a SOT of $u_0 = 30$ m/s with the thermal field. Figure 4 shows one example of the magnetization reversal process at $T = 300$ K. When $\tau = 0$ ns, the magnetic moments canted slightly in various directions from the −y-direction under the influence of the thermal fields (Fig. 4(a)). The magnetic moments at various positions began to rotate (Fig. 4(b)-4(e)), pointing in the +y-direction at $\tau = 0.4$ ns (Fig. 4(f)). The magnetization reversed faster than that at $T = 0$ K. Moreover, the magnetic moment movements during the magnetization reversal process and the magnetization reversal time (τ_r) differed among the various samples.

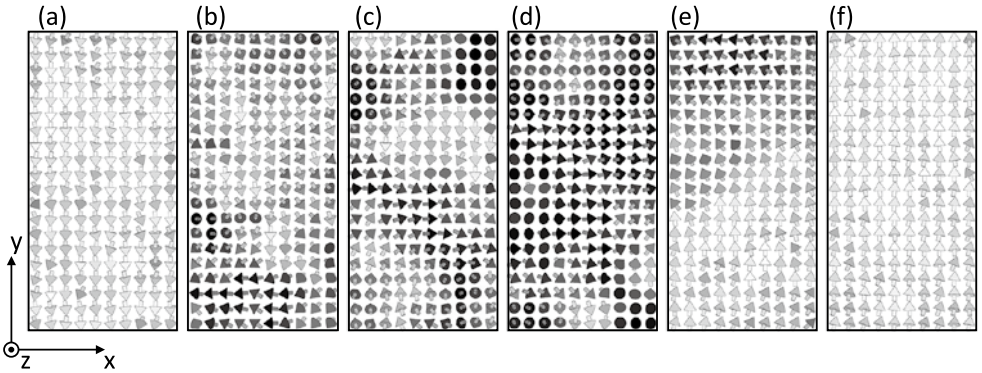

Fig. 4. Snapshots of the magnetization reversal process of the film at 300 K at τ = (a) 0, (b) 0.1, (c) 0.2, (d) 0.25, (e) 0.3, and (f) 0.4 ns; each small arrow indicates the direction of the magnetic moment.

Figure 5(a)-5(e) shows the frequency of the magnetization reversal time (τ_r) for 5,000 samples and the time-dependence of $\langle m_y \rangle$ for three specific samples, namely, the fastest reversal (medium solid curve), the reversal closest to the averaged (τ_r) for the 5,000 samples $\langle \tau_r \rangle$ (bold solid curve), and the reversal at approximately 1.0 ns (thin solid curve), at $T = 0$, 50, 100, 200, 300, and 400 K. Since the +y-polarized spin was injected, the $\langle m_y \rangle$ became over 0.97 even at 400 K when the magnetization reversed. Therefore, we used the above definition of the magnetization reversal time. $\langle m_y \rangle$ at $T = 0$ is represented by the dashed curve in Fig. 5(a)-5(e); $\langle m_y \rangle$ of 0.97 and $\langle \tau_r \rangle$ are represented by the dotted lines.

When $T = 0$ K, the SOT hardly affected the magnetic moments because they are mostly in the −y-direction at $\tau = 0$, as shown in Fig. 2(a). Consequently, the initial response of the magnetization reversal was miniscule. The effect of the SOT increased with increasing τ, after which the magnetization reversed at $\tau = 0.61$ ns. Meanwhile, using the thermal fields, the initial response of magnetization reversals accelerated, as each magnetic moment cants from the −y-direction at $\tau = 0$, as shown in Fig. 2(b)-2(f). Consequently, in most samples, the

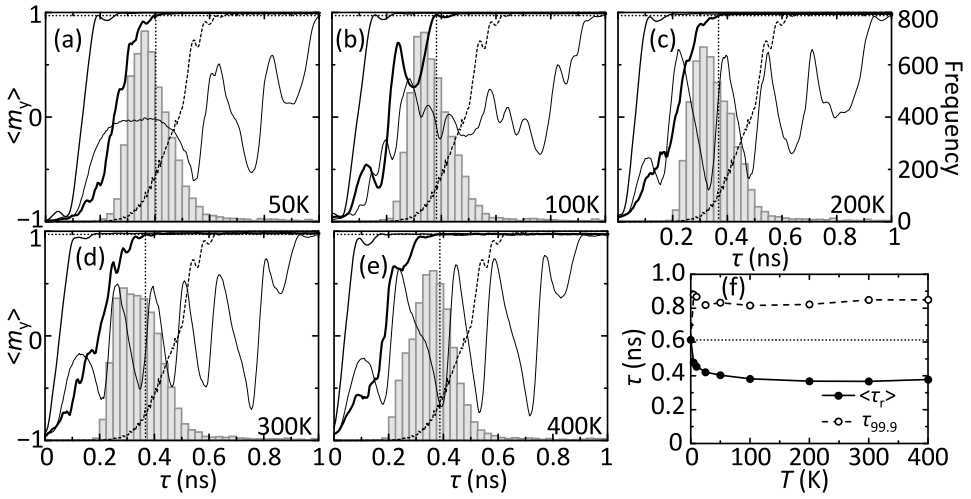

Fig. 5. The magnetization time-dependence of the specific magnetization reversal processes and the frequency of the magnetization reversal time τ_r for 5,000 samples at (a) $T=50$, (b) 100, (c) 200, (d) 300, and (e) 400 K. The dashed curve in (a)-(e) denotes $\langle m_y \rangle$ at $T=0$ K. (f) The temperature dependence of the averaged magnetization reversal time $\langle \tau_r \rangle$ and the time for magnetization reversal to occur in 99.9% of the samples ($\tau_{99.9}$).

magnetization reversed faster than at 0 K. Moreover, the magnetization reversed quickly in the samples with small $|\langle m_y \rangle|$ at $\tau = 0$. However, in some magnetization reversal processes, the magnetization reversed slowly; in these cases, the magnetization reversed while oscillating, increasing the reversal time τ_r.

Figure 5(f) shows the averaged reversal time for 5,000 samples $\langle \tau_r \rangle$ and the time in which the magnetization reversal for 99.9% of the samples occurred ($\tau_{99.9}$) by applying the log-normal fraction. $\langle \tau_r \rangle$ for $T>0$ K was less than 0.61 ns for $T=0$ K, decreasing with increasing temperature up to approximately 100 K before plateauing above 100 K. However, $\tau_{99.9}$ was approximately 35% larger than τ_r at $T=0$ K. The T-dependence of $\tau_{99.9}$ was small.

The reversal time increased owing to the oscillation of the magnetization. However, the magnetization dynamic during the reversal process was not measured experimentally. Such oscillation may be the cause of the sample dependence of the SOT-induced magnetization reversal in the experiment.

4 Conclusions

We investigated the influence of the thermal fields on the magnetization reversal of the permalloy thin film owing to the SOT using micromagnetic simulations. The thermal fields changed the magnetization reversal from symmetric to asymmetric. We found that the initial magnetization reversal response was accelerated under the influence of thermal fields in most samples. Consequently, the averaged magnetization reversal time $\langle \tau_r \rangle$ decreased. However, several samples exhibited exceptional oscillatory behavior of the magnetization during the reversal and the reversal time increased. This increase is a negative result for memory applications. As a future issue, we must determine how to reduce such magnetization

oscillation.

Acknowledgment

This work was supported by the Japan Society for the Promotion of Science KAKENHI Grant Number JP20H02607 and the Kansai University Fund for Supporting Outlay Research Centers 2020.

References

1) J. C. Slonczewski, Current-driven excitation of magnetic multilayers, *Journal of Magnetism and Magnetic Materials,* **159**, L1-L7 (1996).
2) L. Berger, Emission of spin waves by a magnetic multilayer traversed by a current, *Physical Review B*, **54**, 9353 (1996).
3) J. E. Hirsch, Spin Hall effect, *Physical Review Letters*, **83**, 1834-1837 (1999).
4) T. Jungwirth, J. Wunderlich, and K. Olejník, Spin Hall effect devices, *Nature Materials*, **11**, 382-390 (2012).
5) J. Katine, F. Albert, R. Buhrman, E. Myers, and D. Ralph, Current-driven magnetization reversal and spin-wave excitations in Co/Cu/Co pillars, *Physical Review Letters,* **84**, 3149 (2000).
6) A. V. Khvalkovskiy, V. Cros, D. Apalkov, V. Nikitin, M. Krounbi, K. A. Zvezdin, A. Anane, J. Grollier, and A. Fert, Matching domain-wall configuration and spin-orbit torques for efficient domain-wall motion, *Physical Review B*, **87**, 020402(R) (2013).
7) C. Song, R. Zhang, L. Liao, Y. Zhou, X. Zhou, R. Chen, Y. You, X. Chen, and F. Pan, Spin-orbit torques: Materials, mechanisms, performances, and potential applications, *Progress in Materials Science*, **118**, 100761 (2021).
8) Y. Nakatani, Y. Uesaka, and N. Hayashi, Direct Solution of the Landau-Lifshitz-Gilbert Equation for Micromagnetics, *Japanese Journal of Applied Physics*, **28**, 2485 (1989).
9) S. Zhang and Z. Li, Roles of Nonequilibrium Conduction Electrons on the Magnetization Dynamics of Ferromagnets, *Physical Review Letters*, **93**, 127204 (2004).
10) M. A. W. Schoen, J. Lucassen, H. T. Nembach, B. Koopmans, T. J. Silva, C. H. Back, and J. M. Shaw, Magnetic properties in ultra-thin 3d transition metal alloys II: Experimental verification of quantitative theories of damping and spin-pumping, *Physical Review B*, **95**, 134411 (2017).
11) M. Buess, T. Haug, M. R. Scheinfein, and C. H. Back, Micromagnetic Dissipation, Dispersion, and Mode Conversion in Thin Permalloy Platelets, *Physical Review Letters*, **94**, 127205 (2005).
12) D. X. Niu, X. Zou, J. Wu, and Y. B. Xu, Anisotropic magnetization reversal in 30 nm triangular FeNi dots, A*pplied Physics Letters*, **94**, 072501 (2009).
13) W. F. Brown, Jr., Thermal fluctuations of a single-domain particle, *Physical Review*, **130**,

1677 (1963).

14) P. Langevin, Sur la théorie du mouvement brownien, *C. R. Acad. Sci. Paris.*, **146**, 530 (1908).

15) S. Honda and H. Itoh, Micromagnetics simulation for magnetization switching of permalloy films with pure spin current injection, *Journal of Nanoscience and Nanotechnology*, **12**, 8662 (2012).

16) A. V. Khvalkovskiy, V. Cros, D. Apalkov, V. Nikitin, M. Krounbi, K. A. Zvezdin, A. Anane, J. Grollier, and A. Fert, Matching domain-wall configuration and spin-orbit torques for efficient domain-wall motion, *Physical Review B*, **87**, 020402(R) (2013).

17) Y. Yamaki, S. Honda, and H. Itoh, Spin injection into ferromagnetic metal from hevy metal owing to spin Hall effect, *Science and technology reports of Kansai University*, **64**, 51 (2022).